

**Trapping bound water within polymer electrolyte membrane by
calcium phosphotungstate for efficient CO₂ capture**

By Yifan Li,^a Qingping Xin,^{a,b} Shaofei Wang,^{a,b} Zhizhang Tian,^{a,b} Hong Wu,^{a,b} Ye

Liu,^{a,b} and Zhongyi Jiang*^{a,b}

a. Key Laboratory for Green Chemical Technology of Ministry of Education, School of Chemical Engineering and Technology, Tianjin University, Tianjin 300072, China.

b. Collaborative Innovation Center of Chemical Science and Engineering (Tianjin), Tianjin 300072, China.

Experimental

Materials and chemicals: Pebax(R) MH 1657 was purchased from Arkema (French). Phosphotungstic acid was purchased from Aladdin Reagent Co., Ltd. (China). CaCl_2 , $\text{Ca}(\text{NO}_3)_2 \cdot 4\text{H}_2\text{O}$ and ethanol were purchased from Tianjin Guangfu Fine Chemical Research Institute (Tianjin, China). All chemicals were of reagent grade or higher, and were used without further purification.

Synthesis of $\text{Ca}_{1.5}\text{PW}$: $\text{Ca}_{1.5}\text{PW}$ was synthesized via a double-replacement reaction: $\text{H}_3\text{PW} + 1.5\text{Ca}(\text{NO}_3)_2 \rightarrow \text{Ca}_{1.5}\text{PW} + 3\text{HNO}_3$. A certain amount of $\text{Ca}(\text{NO}_3)_2$ solution (3 M) was added into 1M phosphotungstic acid solution drop by drop. By heating the mixture of reactants in a 95 °C oven for 6 h, the by-product, HNO_3 , was thermally decomposed and the synthesis reaction was allowed to be completed. A high yield about 96% was achieved by regarding H_3PW as the benchmark reactant.

Measurement of $\text{Ca}_{1.5}\text{PW}$ solubility: Excessive amount of $\text{Ca}_{1.5}\text{PW}$ was added into water to form saturated solution at different temperature. Each solution was further dried and the derived crystal grains were completely dehydrated at 150 °C under vacuum for over 24 h, and the weight of the anhydrous salt was measured and then the solubility of $\text{Ca}_{1.5}\text{PW}$ was calculated.

Membrane preparation: Pebax was dissolved in ethanol/water (70/30 wt%) under mild mechanical stirring (with reflux) at 80 °C for 3 h to obtain 5 wt% homogeneous solution. After cooling the solution to ambient temperature, a certain amount of $\text{Ca}_{1.5}\text{PW}$ was dissolved into the solution followed by 2 h stirring. The molar ratio of Ca^{2+} to ethylene oxide (EO) unit was controlled at 0, 1:240, 1:120, 1:60 and 1:30, respectively (Further increase of salt content will result in failure of membrane formation). After removing bubbles, the homogeneous solutions were cast onto Teflon petri dishes and then dried under ambient conditions for 24 h. The membranes were further annealed in a vacuum oven at 45 °C for three days to remove the residual solvent. The resultant membranes were designated as Pebax, where salt was absent, or Pebax- $\text{Ca}_{1.5}\text{PW}$ (X), where X means the molar ratio of Ca^{2+} to ethylene oxide (EO) unit. The thickness of all membranes was controlled within the range of 80–90 μm .

Measurement of total water, free water and bound water: Water uptake and water state were determined following the reported procedure. Each membrane was weighed to determine the “humidified” weight (m_1 , mg) after gas permeation, and then heated at 100 °C in a vacuum oven

for 6 h to remove free water. The membranes were reweighed (m_2 , mg) and further dried under vacuum at 150 °C for another 6 h. The completely dried membranes were weighed again to determine their “dried” weight (m_0 , mg). In this way, the content of total water (W_t , %), free water (W_f , %) and bound water (W_b , %) were calculated based on the following equations:

$$W_t = (m_1 - m_0) / m_0 \times 100\%$$

$$W_f = (m_1 - m_2) / m_0 \times 100\%$$

$$W_b = (m_2 - m_0) / m_0 \times 100\%$$

Measurement and prediction of membrane density: Experimental values of membrane density were determined at 25 °C by the buoyancy method using an electronic balance (OHAUS®, CP224C) equipped with density determination kit. Silicon oil with known density ($\rho_0=0.972$ g/cm³) was selected as the auxiliary liquid. Experimental values of density (ρ_B) were calculated by the following equation:

$$\rho_B = \frac{M_A}{M_A - M_L} \rho_0$$

where M_A and M_L are the membrane weight in the air and in the liquid, respectively. Membrane density was also predicted by additive model. Notably, the density of humidified membrane was predicted by assuming that Ca_{1.5}PW was completely or partially dissolved by the adsorbed water, depending on the solubility and content of Ca_{1.5}PW. If Ca_{1.5}PW was completely dissolved, membrane density was calculated by assuming unsaturated Ca_{1.5}PW solution as the additive. If Ca_{1.5}PW was partially dissolved, membrane density was calculated by assuming saturated Ca_{1.5}PW solution and the residual Ca_{1.5}PW crystal as the two additives. The density of Ca_{1.5}PW solution was obtained by measuring the weight and volume of a certain amount of Ca_{1.5}PW solution, of which the Ca_{1.5}PW concentration was determined on the basis of the assumed Ca_{1.5}PW solution within membrane. In this way, the calculated density of humidified membrane could be calibrated by considering the effect of binary interactions between Ca_{1.5}PW and water.

Membrane characterizations: Thermal properties of samples were measured under nitrogen atmosphere by Differential Scanning Calorimetry (DSC) module (DSC 200F3, NETZSCH), with the temperature rising from -70 to 250 °C at a heating rate of 10 °C/min. The chemical structure of membrane was characterized by Nicolet-560 Fourier transform infrared spectrometer (FT-IR) with scan range of 4000–400 cm⁻¹. The crystalline structures of membranes were determined using

wide-angle X-ray diffraction (WAXD) in the range of 10–50° at the speed of 10°/min (Rigaku D/max 2500 v/pc, CuK 40 kV, 200 mA, $\lambda=1.5406 \text{ \AA}$). Fractional free volume (*FFV*) was calculated based on the density data following the previous method.¹

Gas permeation experiments: Single CO₂, CH₄, N₂ and binary CO₂–CH₄ (30vol%:70vol%), CO₂–N₂ (10vol%:90vol%) gas permeation experiments were conducted based on the conventional constant pressure/variable volume technique. The details of the apparatus can be found in our previous work.¹ N₂ was selected as sweep gas when no N₂ existed in feed gas, while CH₄ was utilized as sweep gas to determine the permeability of N₂. In a typical measurement, 3 bar of feed gas was firstly introduced into a water bottle to be saturated with water vapor, and then passed through an empty bottle to remove the residual water. The humidification temperature for feed gas was set 10 °C higher than that of the membrane cell. Meanwhile, the sweep gas was humidified at the same temperature of membrane cell. The flow rate and composition of sweep gas were recorded every 5 minutes until they no longer varied with time. For comparison, dry-state gas permeation experiments were also conducted, in which case the feed gas and sweep gas were directly introduced into the membrane cell. The compositions of the feed, retentate, and permeate were measured using gas chromatography. The permeability (P_i , Barrer, 1 Barrer=10⁻¹⁰ cm³(STP)/cm² s cmHg) of either gas was obtained from the average value of at least 3 tests by the following equation:

$$P_i = \frac{Q_i l}{\Delta p_i A}$$

where Q_i is the volumetric flow rate of gas ‘i’ (cm³/s) at standard temperature and pressure (STP), l is the membrane thickness (cm), Δp_i is the transmembrane partial pressure difference of gas ‘i’ (cmHg), and A is the effective membrane area (12.56 cm²). The ideal selectivity (α_{ij}) was calculated by equation (2):

$$\alpha_{ij} = \frac{P_i}{P_j}$$

Since the permeate side is maintained at ambient pressure, the mixed-gas separation factor could be also calculated by this equation.

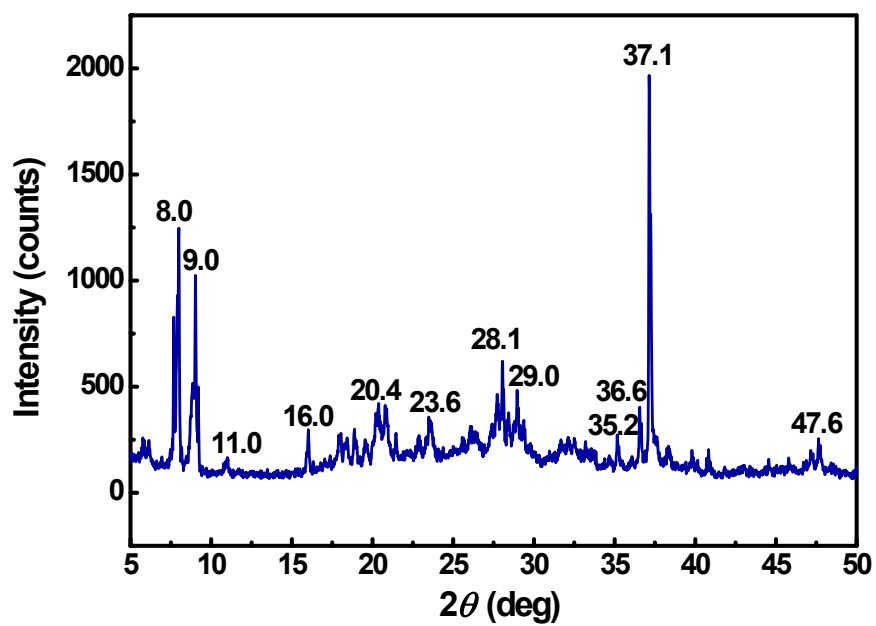


Fig. S1 WAXD spectra of the synthesized Ca_{1.5}PW powder

Fig. S1 shows the Keggin-type characteristic peaks for PW³⁻ at 2=7–10°, 16–23°, 25–30° and 31–38°, respectively, indicating the successful synthesis of Ca_{1.5}PW. ²

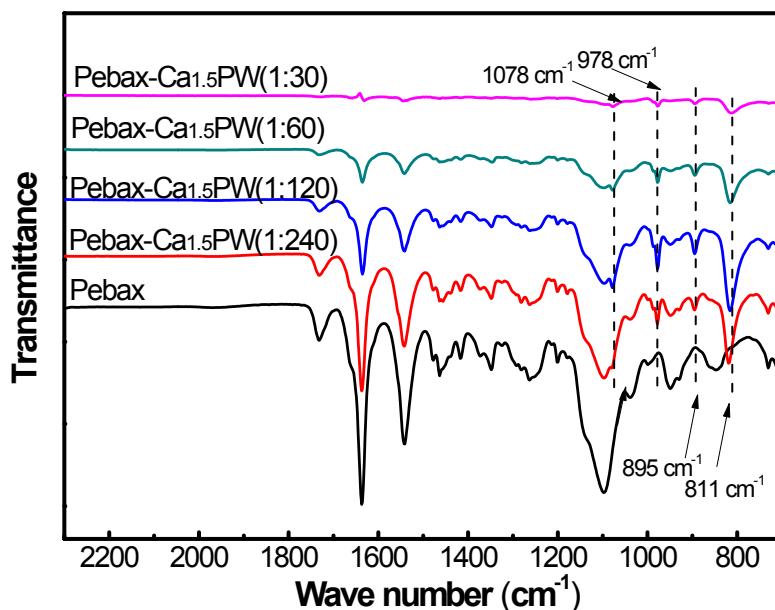


Fig. S2 FTIR curves of Pebax and Pebax–Ca_{1.5}PW membranes

As shown in **Fig. S2**, the characteristic bands assigned to PW³⁻ are observed at 1078 cm⁻¹, 978 cm⁻¹, 895 cm⁻¹, and 811 cm⁻¹, respectively.³⁻⁵ With the addition of Ca_{1.5}PW content, the absolute intensity of these bands firstly increases and then decreases. However, compared to the bands for Pebax (amide-I at 1637 cm⁻¹, amide-II at 1542 cm⁻¹ and ether bond vibration at 1101 cm⁻¹), the relative intensity of the characteristic bands for PW³⁻ actually increases with the addition of Ca_{1.5}PW. The sharp decrease of absolute band intensity for Pebax at high Ca_{1.5}PW content lies in the fact that the actual content of Ca_{1.5}PW in membrane is already 39.5 wt% and 57.6 wt%. The synchronous decrease of the absolute band intensity for PW³⁻ can be interpreted by the delocalization of the electron cloud of W–O bonds towards the C–O bonds.

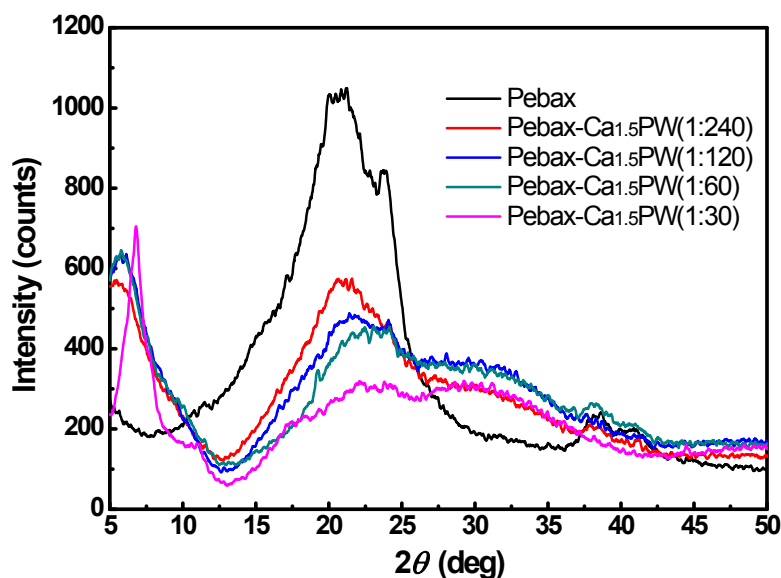


Fig. S3 WAXD spectra of Pebax–Ca_{1.5}PW membranes

The absence of the characteristic sharp peaks for PW³⁻ (see **Fig. S1**) in **Fig. S3** illustrates that Ca_{1.5}PW does not form crystal within membrane. Instead, it complexes with Pebax and achieves a molecular level dispersion. A notable new peak is observed within the 2θ range of 5–7 °, indicating the formation of a hybrid semi-crystalline phase rich in Ca_{1.5}PW. With the increase of Ca_{1.5}PW content, the 2θ value of the peak increases, and the peak becomes sharpened, from which we infer that the membrane becomes denser by ionic crosslinking. Besides, with the increase of salt content, there is a remarkable decrease of the intensity of the typical wide peak for PA6 phase within the 2θ range of 10–30 °, which is reasonably attributed to the disruption of PA6 semi-crystalline phase by Ca_{1.5}PW.

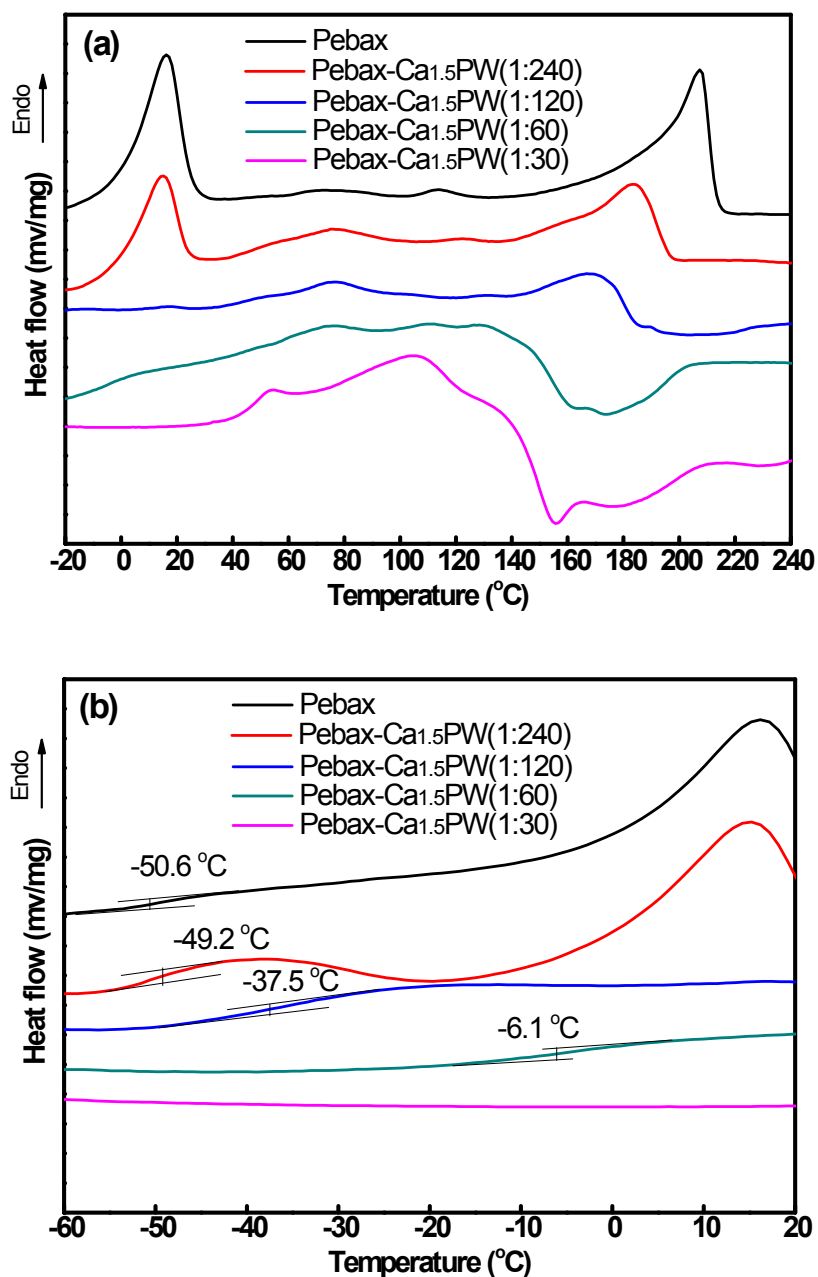


Fig. S4 DSC curves of Pebax and Pebax–Ca_{1.5}PW membranes: (a) high temperature zone; (b) low temperature zone

Fig. S4a represents the effects of Ca_{1.5}PW on the respective crystalline phase regions of the PEO and PA6 segments of Pebax. Obviously, the crystalline phase regions of PEO segment (characterized by the left peak) and PA6 segment (characterized by the right peak) become completely damaged when Ca²⁺:EO increases up to 1:120 and 1:60, respectively. These results show that Ca_{1.5}PW can significantly complex with both PEO segment and PA6 segment, and the interactions between Ca_{1.5}PW and PEO appears to be relatively stronger. When Ca²⁺:EO is higher

than 1:120, an exothermic heat flow is observed. Considering that any heat flow ascribed to phase change displays endothermic characteristics, the exothermic heat flow can be only interpreted by the degradation of Pebax catalyzed by $\text{Ca}_{1.5}\text{PW}$. With the increase of $\text{Ca}^{2+}:\text{EO}$ from 1:120 to 1:30, the endothermic peak becomes more intense, and the valley temperature becomes lower, which can support the hypothesis that $\text{Ca}_{1.5}\text{PW}$ lowers the thermally degradation temperature and accelerates the degradation process. Since the endothermic peak lies above 120 °C, the membrane is still expected to maintain thermal stability below 100 °C, which is adequate for common operation.

Fig. S4b reflects the effects of $\text{Ca}_{1.5}\text{PW}$ on the chain rigidity of PEO segment. The glass transition temperature (T_g) remarkably increases with the increment of $\text{Ca}^{2+}:\text{EO}$, and the T_g value for Pebax– $\text{Ca}_{1.5}\text{PW}(1:60)$ membrane is already up to -6.1 °C (much higher than that of Pebax– $\text{CaCl}_2(1:60)^1$), demonstrating the strong complexation between PW^{3-} and PEO. Such strong interactions can be also understood by the fact that phosphotungstic acid is often purified by using diethyl ether as extraction solvent. For Pebax– $\text{Ca}_{1.5}\text{PW}(1:30)$ membrane, the T_g cannot be detected, which may be interpreted by the highly crosslinked membrane structure.

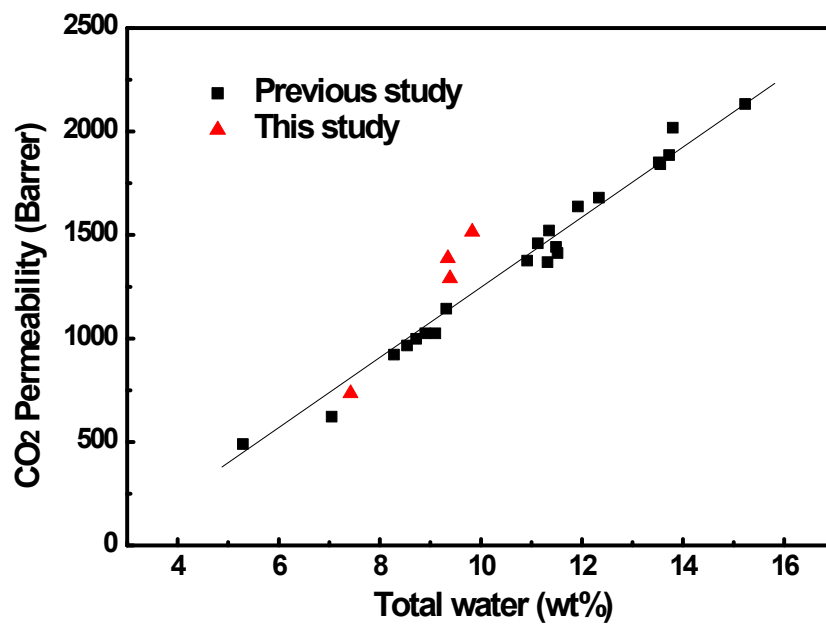


Fig. S5 Correlations between pure-gas permeability and total water content of the membrane based on the previously reported plot from Ref. S1.

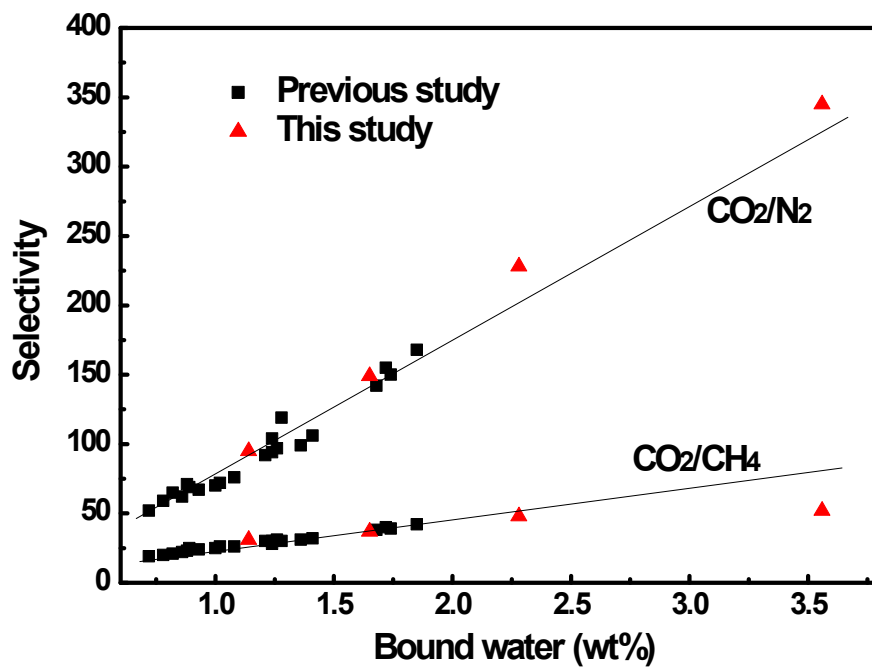


Fig. S6 Correlations between pure-gas CO₂/CH₄, CO₂/N₂ selectivity and bound water content of the membrane based on the previously reported plot from Ref. S1.

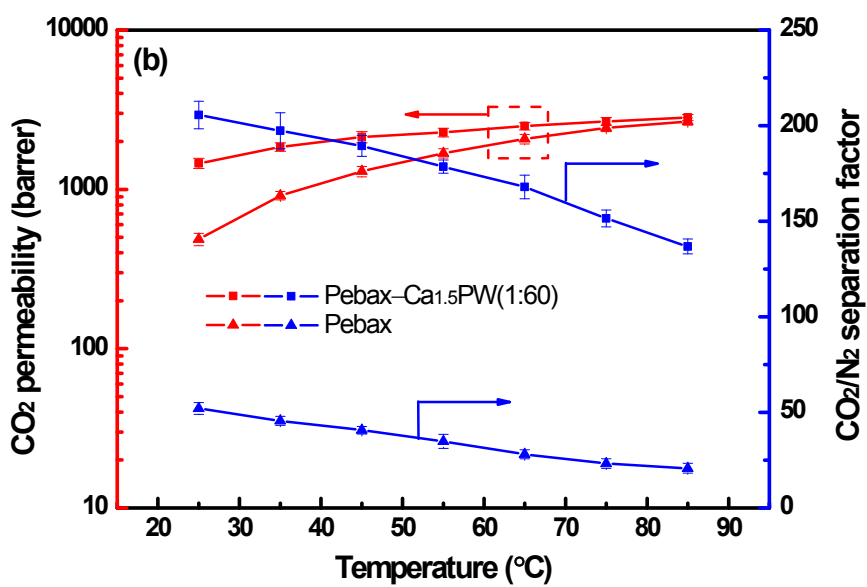
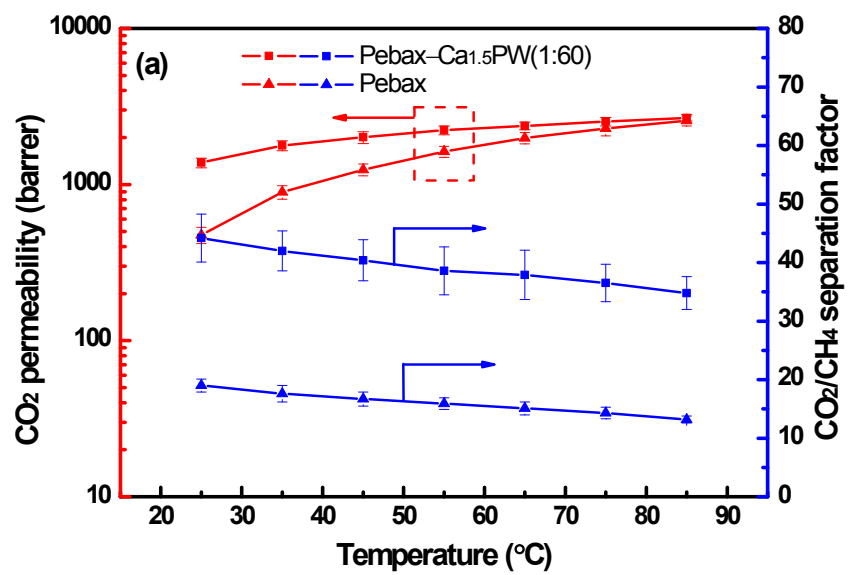


Fig. S7 Effect of operating temperature on CO₂ capture properties of Pebax-Ca_{1.5}PW(1:60) : (a) CO₂/CH₄ separation; (b) CO₂/N₂ separation

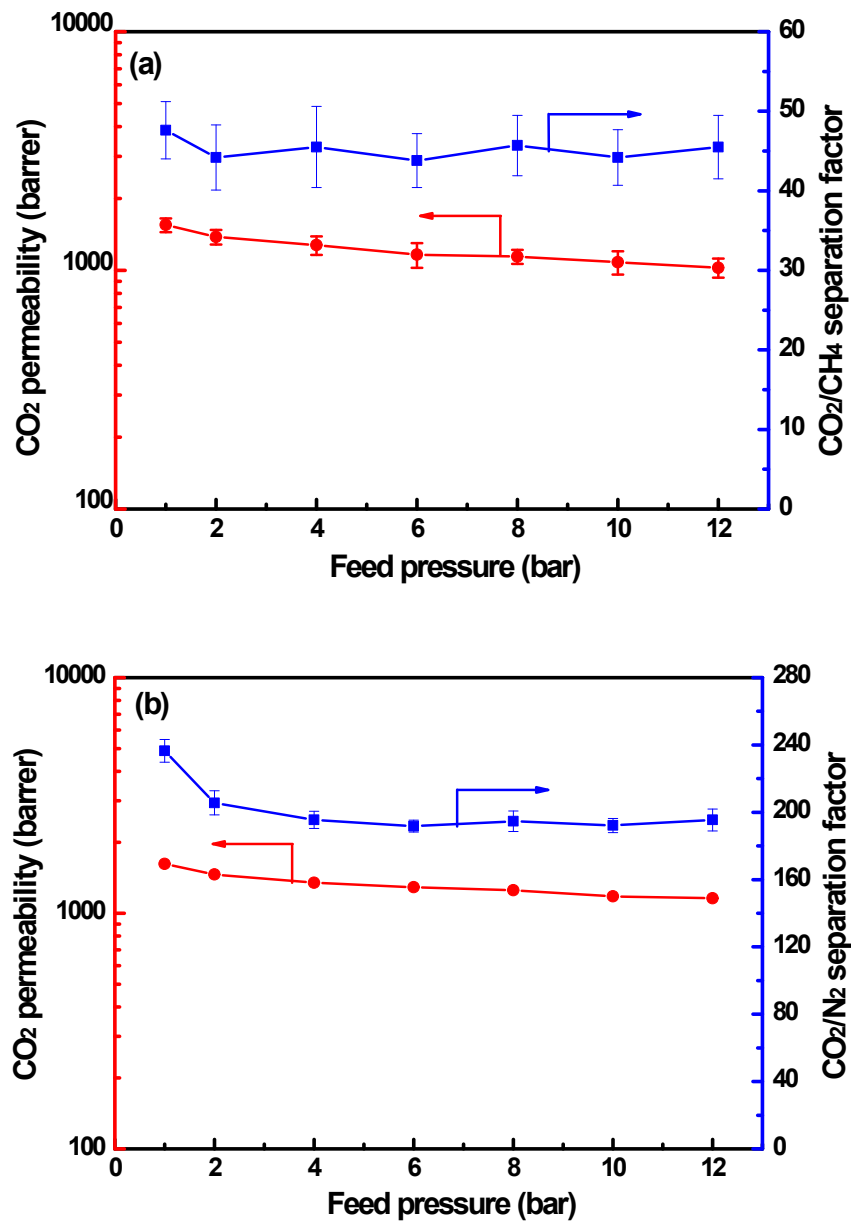


Fig. S8 Effect of feed pressure on CO₂ capture properties of Pebax–Ca_{1.5}PW(1:60) at 25 °C: (a) CO₂/CH₄ separation; (b) CO₂/N₂ separation

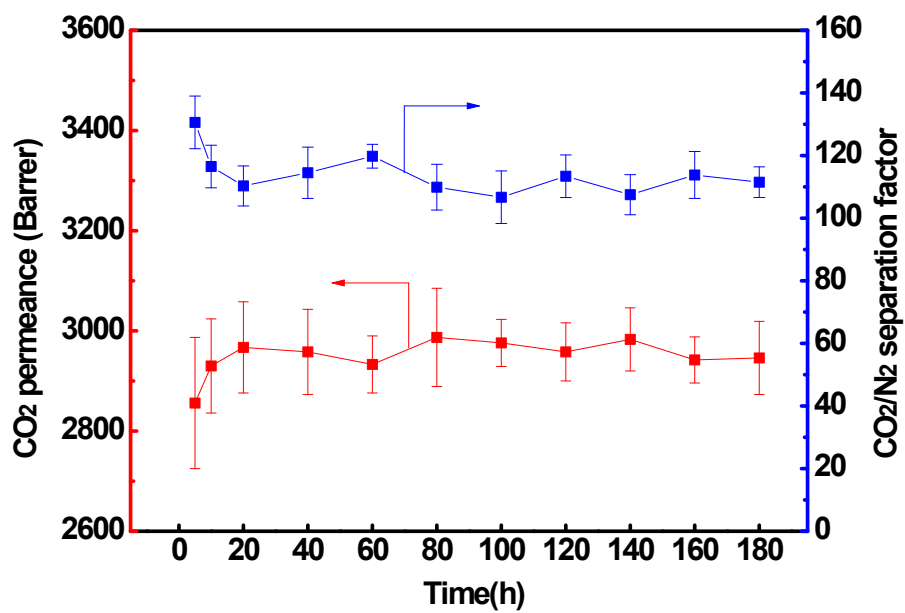


Fig. S9 The long-time mixed-gas separation test of the Pebax–Ca_{1.5}PW(1:30) membrane at 85 °C and 3 bar.

Table S1 Experimental and predicted densities of the dry membranes and humidified membranes ^a

Sample	Dry membrane			Humidified membrane		
	ρ_B	ρ_M	$\rho_B - \rho_M$	ρ_B	ρ_M^b	$\rho_B - \rho_M$
Pebax	1.140±0.005	1.140	0±0.005	1.108±0.004	1.133±0.005	-0.025±0.005
Pebax–Ca _{1.5} PW(1:240)	1.279±0.006	1.277	0.001±0.006	1.247±0.009	1.269±0.013	-0.022±0.014
Pebax–Ca _{1.5} PW(1:120)	1.413±0.007	1.405	0.008±0.007	1.367±0.007	1.406±0.012	-0.038±0.011
Pebax–Ca _{1.5} PW(1:60)	1.659±0.004	1.635	0.023±0.004	1.546±0.013	1.642±0.014	-0.096±0.014
Pebax–Ca _{1.5} PW(1:30)	2.055±0.005	2.014	0.041±0.005	1.933±0.006	2.014±0.013	-0.081±0.010

a. ρ_B and ρ_M mean the densities obtained by buoyancy method and additive model, respectively.

b. Error bar is added because the calculation involves the density of salt solution, which was measured experimentally.

Table S2 Calculated FFV values of the dry membranes and humidified membranes

Sample	FFV _{dry}	FFV _{humidified}	FFV _{humidified} -FFV _{dry}
Pebax	0.126±0.007	0.194±0.012	0.068
Pebax-Ca _{1,5} PW(1:240)	0.121±0.005	0.198±0.013	0.077
Pebax-Ca _{1,5} PW(1:120)	0.114±0.008	0.201±0.015	0.087
Pebax-Ca _{1,5} PW(1:60)	0.102±0.006	0.202±0.017	0.100
Pebax-Ca _{1,5} PW(1:30)	0.088±0.004	0.171±0.011	0.083

Table S3 Comparison of pure-gas permeation properties of the dry membranes and humidified membranes

Sample	Dry membrane			Humidified membrane		
	P_{CO_2}	$\alpha_{\text{CO}_2/\text{CH}_4}$	$\alpha_{\text{CO}_2/\text{N}_2}$	P_{CO_2}	$\alpha_{\text{CO}_2/\text{CH}_4}$	$\alpha_{\text{CO}_2/\text{N}_2}$
Pebax	82±3.8	19±0.3	54±2.6	490±28	19±0.5	52±2.0
Pebax–Ca _{1.5} PW(1:240)	59±2.2	22±1.7	70±3.3	735±31	31±1.6	95±3.0
Pebax–Ca _{1.5} PW(1:120)	55±1.9	25±1.5	65±2.5	1290±29	37±1.3	149±5.2
Pebax–Ca _{1.5} PW(1:60)	49±2.1	28±0.7	42±2.1	1515±25	48±1.0	228±4.0
Pebax–Ca _{1.5} PW(1:30)	34±1.7	29±0.9	21±1.7	— ^a	—	—

a. “—” means the data were not obtained, because the Pebax–Ca_{1.5}PW (1:30) membrane at humidified state is not robust enough to afford the testing pressure difference (3 bar).

The application prospects of Pebax-Ca_{1.5}PW membrane

Pebax–Ca_{1.5}PW membrane exhibits a high CO₂ permeability of 2825 Barrer and a high CO₂/N₂ selectivity of 137 at 85 °C, and the data point is already well above the Robeson upper bound revisited in 2008.⁶ Considering the temperature of flue gas after recycling residual heat usually lies within 110–160 °C, high CO₂ capture performance at 80–100 °C not only eliminates the necessity of cooling down the feed gas to room temperature, but also provides proper temperature difference for condensing a thin water film onto membrane surface,⁷ where the possible defects are expected to be sealed. Pebax–Ca_{1.5}PW membrane also shows weak dependence of CO₂ capture properties on feed pressure (**Fig. S8**), which means that the membrane is also available at elevated pressure. Furthermore, the membrane maintains the separation performance during a 160 h-long mixed-gas separation experiment, and no evidence of membrane deterioration can be observed (**Fig. S9**).

References

1. Y. Li, Q. Xin, H. Wu, R. Guo, Z. Tian, Y. Liu, S. Wang, G. He, F. Pan and Z. Jiang, *Energy Environ. Sci.*, 2014, **7**, 1489-1499.
2. A. Aouissi, Z. A. Al-Othman and A. Al-Amro, *Int. J. Mol. Sci.*, 2010, **11**, 1343-1351.
3. H. Wu, X. Shen, Y. Cao, Z. Li and Z. Jiang, *J. Membr. Sci.*, 2014, **451**, 74-84.
4. M. Huang, W. Chu, X. Liao and X. Dai, *Catal. Lett.*, 2011, **141**, 1670-1676.
5. K. Srilatha, R. Sree, B. L. A. Prabhavathi Devi, P. S. Sai Prasad, R. B. N. Prasad and N. Lingaiah, *Bioresour. Technol.*, 2012, **116**, 53-57.
6. L. M. Robeson, *J. Membr. Sci.*, 2008, **320**, 390-400.
7. M. Poloncarzova, J. Vejrazka, V. Vesely and P. Izak, *Angew. Chem. Int. Ed.*, 2011, **50**, 669-671.